Implementation and Test of Human-Operated and Human-Like Adaptive Impedance Controls on Baxter Robot

Peidong Liang[1,3], Chenguang Yang[1,2,⋆], Ning Wang[1,4], Zhijun Li[2], Ruifeng Li[3], and Etienne Burdet[5]

[1] Centre for Robotics and Neural Systems, School of Computing and Mathematics, Plymouth University, UK
[2] The MOE Key Lab of Autonomous System & Network Control, College of Automation Science and Engineering, South China University of Technology, China
cyang@ieee.org
[3] The State Key Laboratory of Robotics and System, Harbin Institute of Technology, China
[4] Department of Computer Science and Engineering, The Chinese University of Hong Kong, China
[5] Department of Bioengineering, Imperial College of Science, Technology and Medicine, London, UK

Abstract. This paper presents an improved method to teleoperate impedance of a robot based on surface electromyography (EMG) and test it experimentally. Based on a linear mapping between EMG amplitude and stiffness, an incremental stiffness extraction method is developed, which uses instantaneous amplitude identified from EMG in a high frequency band, compensating for non-linear residual error in the linear mapping and preventing muscle fatigue from affecting the control. Experiments on one joint of the Baxter robot are carried out to test the approach in a disturbance attenuation task, and to compare it with automatic human-like impedance adaptation. The experimental results demonstrate that the new human operated impedance method is successful at attenuating disturbance, and results similarly to as automatic disturbance attenuation, thus demonstrating its efficiency.

Keywords: EMG, stiffness estimation, adaptive impedance control, teleoperation.

1 Introduction

Human-like robot control has received increasing research attention in recent years e.g. [1,2], boosted in part by the development of serial elastic actuator (SEA) [3] and variable impedance actuator (VIA) [4]. Inspired by the flexibility humans have to adapt visco-elasticity at the endpoint of their arm, impedance control introduced by Hogan in 1985 aims at controlling mechanical impedance,

⋆ Corresponding author.

M. Mistry et al. (Eds.): TAROS 2014, LNAI 8717, pp. 109–119, 2014.

the relation between force and displacement [5], [6]. Considering how humans can skilfully adapt impedance in various force interactive scenarios, e.g. when using tools, we would like to transfer this flexibility to robots [1]. One possibility to adapt impedance is by using human-like adaptation, e.g. as was developed in [1]. Alternatively, human-like impedance strategies may be achieved using electromyography (EMG) signals to decode impedance in real time, see e.g. [7]. Advantages of teleoperation via EMG include: i) simple and natural control interface which is convenient for teleoperation; ii) low cost sensing EMG signals are easy to be acquired; iii) transparent interaction between human and robot avoiding the delay inherent in providing feedback. In view of these potential advantages, [7] developed a teleimpedance system in which a slave robot is commanded in position from the operator arm position and in impedance from the EMG signals recorded on his or her arm.

This paper proposes to compare these two approaches to adapt impedance in a disturbance attenuation task. A human operator is controlling the position of a robot arm using visual feedback. This robot is subjected to high-frequency external disturbance, that either the robot can attenuate using human-like impedance adaptation [1], or the human operator can attenuate using his EMG. Instead of estimating the stiffness value directly from EMG as in [7], the increment of stiffness value is used to compensate for the potential nonlinear residual error in the linear mapping used in [7]. Furthermore, only the 400-500Hz band of EMG is employed for stiffness estimation [8], which prevent fatigue from affecting the impedance control. An instantaneous amplitude detection algorithm is used to compute stiffness value, which enhances the robustness of EMG processing. The two impedance adaptation methods are tested to teleoperate a Baxter robot arm submitted to external disturbance. The control objective is to maintain a given pose with the Baxter robot in the presence of high frequency external disturbances, for simplicity here in only the shoulder joint.

2 Preliminaries

2.1 Baxter Robot Programming

The Baxter robot used for our experiments, shown in Fig. 1 consists of a torso, 2 DOF head and two 7 DOF arms (shoulder joint: s0, s1; elbow joint: e0, e1; wrist joint: w0, w1, w2), integrated cameras, sonar, torque sensors, and direct programming access via a standard ROS interface. Each joint of the Baxter robot arm is driven by a SEA (illustrated in Fig.1), which provides passive compliance to minimise the force of any contact or impact [9]. ROS (Robot Operating System) SDK is used to control and program the Baxter robot with Baxter RSDK running on Ubuntu 12.04 LTS which is an open source framework with modular tools, libraries, and communications. It simplifies the task of modelling and programming on a wide variety of robotic platforms. In this paper, the robot control is implemented through several sets of nodes and data series of the extracted impedance from human can be sent to the bridge machine for connection between Baxter robot and human. On the human bridge

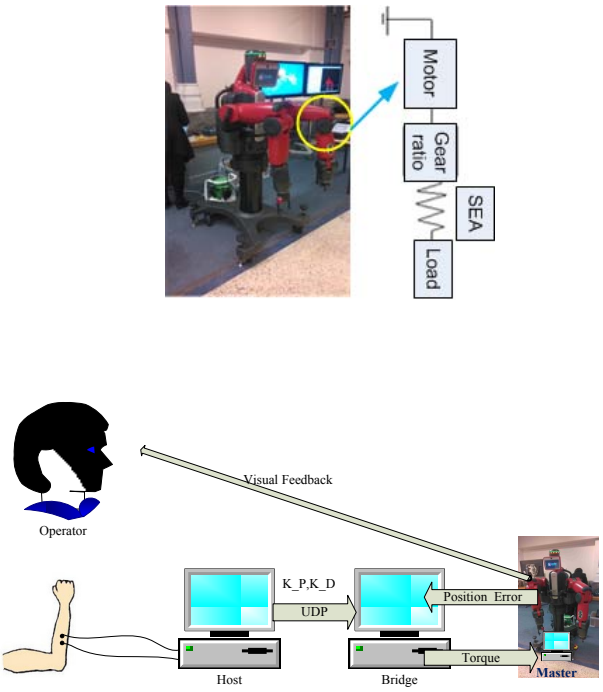

Fig. 1. Experimental setup. Top: Baxter research robot with SEA joints (schematic of SEA shown on the right). Below: Data flow.

machine side, stiffness is computed on the MATLAB 2014a and sent to the bridge machine via UDP, a Python script is set up to receive these data set and build a new node to publish a topic for the robot side via Ethernet. Another interface is built with torque control mode to receive and process human impedance and give feedback to human Data flow is also shown in Fig. 1.

3 Adaptive Impedance Control Methods

3.1 Human-Like Adaptive Impedance Control

Human-like robot control with adaptive impedance was developed in [1] as follows:

$$\tau_u = -\tau_{ff} - \tau_{fb} - L\epsilon + \tau_r \tag{1}$$

where $-\tau_{ff}$ is feedforward torque learned to compensate for the interaction with the environment, $\tau_{fb} = -K_P e - K_D \dot{e}$ plays the role of feedback, with stiffness K_P and damping K_D parameters to be learned during interaction with the environment, and $e = q - q^*, \dot{e} = \dot{q} - \dot{q}^*$ are position and velocity errors relative to the task reference trajectory q^*. $L\epsilon$ denotes the ideal stability margin, and L is a control matrix used to keep robot motion with stability and compliance,

whereas $\epsilon = \dot{e} + ke, k > 0$ is the tracking error. The term τ_r is used to counteract the complexity of robot dynamics and disturbances. The adaptation of stiffness is enabled by the following algorithm (originally proposed in iteration domain in [1], and extended to time domain in [10]).

$$\begin{aligned} \Delta K_P^{t+1} &= Q^t(\epsilon^t e^{tT} - \gamma^t K_P^t) \\ \Delta K_P^{t+1} &= K_P^{t+1} - K_P^t \end{aligned} \tag{2}$$

and adaptation of damping K_D is similar and thus omitted here. Notation t is the current time sampling point and $t+1$ next time sampling point, $Q^t = Q^{t^{\mathrm{T}}}$ is a positive definite gain matrix, and the forgetting factor γ can be simply chosen as a constant coefficient. It has been theoretically and experimentally shown that the algorithm of equation (2) is able to adapt robot impedance in a human-like manner, i.e., when there is large unpredictable external disturbances, the stiffness will increase to compensate for the disturbance, while the disturbance decreases stiffness will be reduced to save control effort.

3.2 Improved Stiffness Estimation Using EMG

According to [11,12], we assume that a linear mapping can be employed to approximate the relationship between rectified EMG amplitude and joint torques. We also consider a potential residual term in addition to the linear mapping such that the relationship between rectified EMG amplitude and joint torques is

$$\tau^t = \sum_{i=1}^{n} \alpha_i \cdot A_{i,t}^a - \sum_{i=1}^{n} \beta_i \cdot A_{i,t}^{aa} + r_\tau^t \tag{3}$$

where α_i, β_i are unknown constant coefficients; τ^t is the joint torque generated by agonist/antagonist muscle pairs involved in the joint motion; $A_{i,t}^a$ and $A_{i,t}^{aa}$ represent the rectified EMG amplitude of the agonist and antagonist muscles, respectively (in this work, we will use the identified temporal envelop of the EMG signal extracted from a certain high frequency band to remove effect caused by muscle fatigue); r_τ^t is the potential non-linear residual term. In order to reduce the effect of the residual error and to simplify the non-linearity, incremental stiffness estimation is introduced by taking a first order difference of above equation:

$$\Delta\tau^{t+1} = \sum_{i=1}^{n} \alpha_i \cdot \Delta A_{i,t+1}^a - \sum_{i=1}^{n} \beta_i \cdot \Delta A_{i,t+1}^{aa} + \Delta r_\tau^{t+1} \tag{4}$$

where $\Delta\tau^t = \tau^{t+1} - \tau^t$ is incremental torque; $\Delta A_{i,t+1}^a = A_{i,(t+1)}^a - A_{i,t}^a$; $\Delta A_{i,t+1}^{aa} = A_{i,(t+1)}^{aa} - A_{i,t}^{aa}$ are incremental EMG amplitude; and we assume $\Delta r_\tau^{t+1} = r^{t+1} - r^t \approx 0$. Following [11,12], we assume the joint stiffness can be approximated by the following equation by taking into consideration of a potential residual term

$$K_P^t = \sum_{i=1}^{n} |\alpha_i| \cdot A_{i,t}^a + \sum_{i=1}^{n} |\beta_i| \cdot A_{i,t}^{aa} + r_K^t \tag{5}$$

where K^t denotes the stiffness generated by muscles involved at current time t, and r_K^t is the non-linear residual term. By taking a first order difference of above equation, we propose a method to estimate incremental stiffness of human arm as described in (6). On one side, this method would help to overcome the effect caused by the potential non-linear residual item. On the other side, by transferring estimated incremental stiffness to the robot, possible accident caused by sudden fall of stiffness on robot would be avoided. This may happen when the initial stiffness on robot is higher than the initial stiffness estimated on human operator.

$$\Delta K_P^{t+1} = \sum_{i=1}^{n} |\alpha_i| \cdot \Delta A_{i,t+1}^{aa} + \sum_{i=1}^{n} |\beta_i| \cdot \Delta A_{i,t+1}^{a} \tag{6}$$

where $A_{i,t}^{aa}$ is the detected amplitude of EMG of the ith antagonistic muscle at the current time instant t, and $A_{i,t}^{a}$ the amplitude of agonistic muscle, and $\Delta A_{i,t+1}^{aa} = A_{i,t+1}^{a} - A_{i,t}^{a}$, $\Delta A_{i,t+1}^{a} = A_{i,t+1}^{a} - A_{i,t}^{a}$. Instead of using amplitude of rectified raw EMG, we will perform signal processing to detect instantaneous amplitude $A_{i,t}^{aa}$ and $A_{i,t}^{a}$, using frequency band decomposition and envelop detection. This will be detailed in section 3.3.

3.3 Signal Decomposition and Amplitude Extraction of EMG Signals

EMG signals are non-invasive and generated in muscle activities, representing muscle tension, joint force and stiffness variation [13], which are a linear summation of a compound of motor-unit action potentials (MUAPs) trains triggered by motor units and correlative with force according to [8]. In this paper, the EMG signal is processed as a multi-component amplitude and frequency modulating (AM-FM) signals due to its sufficiently small-band width [14] described by

$$s^t = \sum_{k=0}^{K} A_k^t \cos \Theta_k^t + \eta^t \tag{7}$$

where A_k^t denotes the instantaneous amplitude of the kth EMG component, corresponding to A_i^a or A_i^{aa} in Eq. (5) and Θ_k^t denotes its instantaneous phase. η^t denotes residual errors caused by disturbance, modelling error and finite summation etc. The instantaneous amplitude A^t identified using (7) according to [14] can be regarded as temporal envelop of the EMG signal extracted from a certain frequency band (refer to Fig. 3), and the frequency band of 400-500Hz is used in this paper. In this manner, we would have less variation of EMG amplitude in comparison to the amplitude of raw EMG , and avoid muscle fatigue effect which is mainly embedded in low frequency EMG band [8]. In addition, as the instantaneous amplitude detected is always positive [14], the rectification can be omitted. In this work, NI USB6210 (16 inputs 16bit, 250KS/s, and multi-function I/O), and 8 channels EMG Pre-Amplifier are used for detecting EMG signals with MATLAB 2014a 32bit data acquisition toolbox. The sampling rate is 2000Hz with 200 data every 0.1s interval for real time processing.

3.4 Human-Operated Impedance Control Experimental Setup

The whole teleoperation system design is shown in Fig. 2. It consists of the following components: EMG signals acquiring and processing, stiffness estimation, communication between host and master machine, and adaptive controller on Baxter robot. In this paper we only consider controlling a single shoulder (s1) joint of Baxter robot using wrist flexion/extension joint of human operator. EMG signals are gathered through electrodes and filtered, then the stiffness

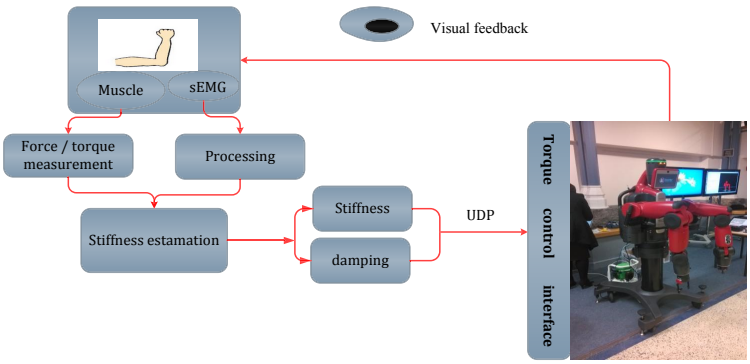

Fig. 2. Overall scheme of teleoperation system

and damping are estimated from EMG with the reference endpoint force measured by a dynamometer. We use UDP to transfer data from host machine with MATLAB2014a 32bit to the master machine which is an interface programmed in Python for interacting with Baxter robot. For simplicity of implementation, only feedback part τ_{fb} in the controller (1) is used in the experiment, where K_P is obtained from (6) and K_D is set as

$$K_D = \sigma \cdot \sqrt{K_P} \tag{8}$$

where $\sigma = 0.2$ is a properly chosen coefficient for the SEA driven joints. The robot will tend to become stable with the increase of impedance. The human operator can adapt impedance using visual feedback, i.e., when the disturbances are increasing, human operator stiffens his/her muscles and relaxes if the robot is little disturbed.

4 Experimental Results

Our experiment compared human-like automatic impedance adaptation and human operated adaptation of impedance. One adult male human operator is performing the experiment. His wrist flexor carpi radialis and extensor carpi radialis were selected to extract stiffness to control Baxter robot impedance in its shoulder (s1) joint.

4.1 Incremental Stiffness Estimation from EMG

Fig. 3 shows an example of EMG signal processing using AM-FM demodulation method described in section 3.3. The bottom panel shows the EMG signal extracted in the 400-500Hz frequency band, and the detected instantaneous amplitude as the temporal envelop of the signal.

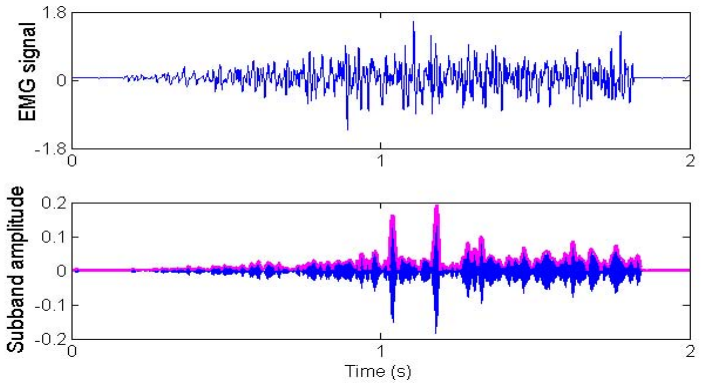

Fig. 3. Top: the raw EMG signal. Bottom: its sub-band of 400-500Hz in blue with identified instantaneous amplitude in pink.

In this preliminary study, only EMG signals of two channels measured from a pair of muscles on wrist were used in the experiments, so equation (6) can be as an equation with only two parameters α and β to identify. For the purpose of calibration, the human operator exerts three different constant forces: $10N$ (wrist extension), $40N$ (wrist flexion) and $50N$ (wrist flexion) against a dynamometer. Before recording EMG data, Labview interface was started to ensure that the signal is at a standard low noisy level, then the human operator's wrist maintains a constant force/torque. When the signals remained stable, recording started using MATLAB2014a 32bit data acquisition toolbox. When the operator maintains the desired force, the lever of force was measured as $0.05m$ and thus torques corresponding to the three forces were $-0.5N \cdot m$, $2N \cdot m$ and $2.5N \cdot m$, respectively.

Fig.4 illustrates the calibration process. The raw EMG signals of the pair of muscles when maintaining the three different levels of torque were measured and shown in 4(a), (b) and (c), respectively. The identified instantaneous amplitudes of these signals extracted from 400-500Hz band are shown in 4(d), (e) and (f). For ease of computation, we took amplitude differences between amplitudes shown in 4(e) and (d), 4(f) and (d), which are shown in 4(g) and (h), instead of taking difference between different sampling points as in (4). The average of the EMG amplitude differences shown in 4(g) and (h) are $0.0112, -0.0040$ and $(0.0095, -0.0035)$, shown in Fig. (4)(i). As the torque differences are $2.5N \cdot m$ and $3N \cdot m$, the values of α and β are calculated as $\alpha = -2708.3$ and $\beta = 8208.3$.

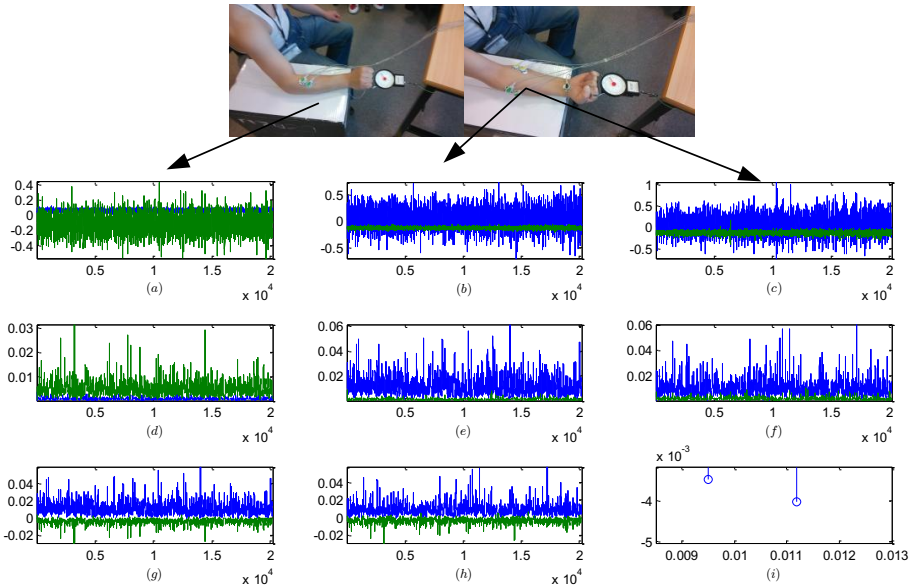

Fig. 4. Calibration process: (a), (b) and (c) denote the raw EMG signals of agnostic and antagonistic muscles of wrist flexion/extension when maintaining -10N (extension), 40N (flexion) and 50N respectively; (d), (e) and (f) are the identified instantaneous amplitude of the 400-500Hz sub-band signals extracted from raw signals shown in (a), (b) and (c); (g) and (h) denote the difference of the amplitudes between (e) and (d), (f) and (d), respectively; (i) denotes the average values of the amplitude difference shown in (g) and (h) (x-axis:flexion muscle, y: extension muscle)

4.2 Comparison between Human-Like Control and Human-Operated Control

Two comparative experiments were carried out to test the proposed methodology in torque control mode of the Baxter robot. Only shoulder joint (s1) was used to implement the adaptive control, while the rest joints stiffness's and damping rate are set with properly chosen values to avoid resonance. Here, the values were: stiffness(N/m)(s0: 400.0; e0: 50; e1: 200; w0: 50; w1:25; w2: 20). Damping rates are set according to Eq. (8). The initial stiffness value for s1 was 15 N/m. Fig. 5 (a) and (b) show the human-like control and human operated control experimental results on Baxter robot under external high frequency disturbances, respectively. Equations (2) and (6) are used to generate the incremental values of stiffness shown in the middle panels of Fig. 5 (a) and (b), respectively. The summation of these values of incremental stiffness along sample points contribute to the variation of the values of stiffness shown in the first panel of Fig. 5 (a) and (b). Note that the summations along the sample points is sampling frequency times the integration along time. From the performance of attenuation of disturbances as shown in the third panels of Fig. 5 (a) and (b), we see that human

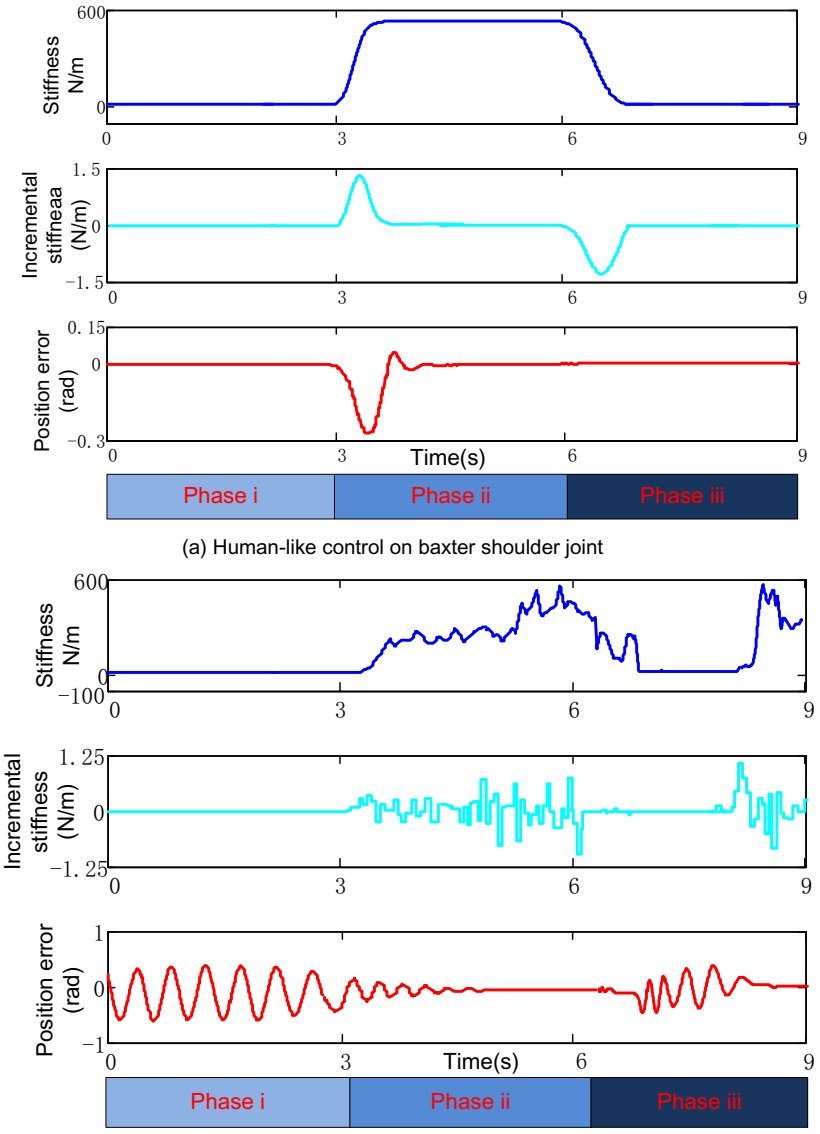

Fig. 5. Comparison between human-like control and human-operated control: (a) Human-like control on Baxter (s1) joint with three phases: i) robot should relaxes in the absence of external disturbance; ii) robot shoulder stiffens up when the high frequency external disturbance is applied; iii) robot shoulder relaxes again when the disturbances are removed. (b) Human-operated control on Baxter (s1) joint with three phases: i) human operator keeps wrist relaxed when of high frequency external disturbances are applied on the Baxter robot; ii) human operator stiffens up his wrist joint to increase impedance on the Baxter robot; iii) human operator relaxes and then stiffens up his wrist joint when the external disturbances are applied.

operated online impedance control via EMG is as good as automatic impedance adaptation to attenuate external perturbations, in turn showing its efficiency.

5 Conclusion

The paper proposed an improved strategy of EMG based incremental stiffness estimation without calibration and nonlinear residual errors for robot teleoperation which requires high dynamic performances in unknown environment. A telecontrol disturbance attenuation experiment was designed to compare this improved algorithm with automatic human-like adaptation of impedance. Results show that the proposed methodology is efficient in teleoperation with human skills transferring to robot in unknown environment, as can be seen in the attached illustrative videos[1]. Using human operated impedance control brings more flexibility than automatic disturbance attenuation, but requires appropriate visual feedback and attention from a human operator.

Acknowledgement. The authors thank Dr. Hai Li who built the amplifier for EMG data collection, Dr Ali Al-Timemy who helped to set up the EMG data capture interface and Zhangfeng Ju who helped to set up the experiment. This work was supported in part by EPSRC grants EP/L026856/1 and EP/J004561/1, Royal Society grants RG130244, IE130681 and JP100992; foundation of Chinese MOE Key Lab of Autonomous Systems and Networked Control grants 2012A04 and 2013A04; and EU-FP7-ICT-601003 BALANCE projects.

References

1. Yang, C., Ganesh, G., Haddadin, S., Parusel, S., Albu-Schaeffer, A., Burdet, E.: Human-like adaptation of force and impedance in stable and unstable interactions. IEEE Transactions on Robotics 27(5), 918–930 (2011)
2. Yang, C., Li, Z., Burdet, E.: Human like learning algorithm for simultaneous force control and haptic identification. In: 2013 IEEE/RSJ International Conference on Intelligent Robots and Systems (IROS), pp. 710–715 (November 2013)
3. Pratt, G.A., Williamson, M.M.: Series elastic actuators. In: Proceedings of the 1995 IEEE/RSJ International Conference on Intelligent Robots and Systems 1995, Human Robot Interaction and Cooperative Robots, vol. 1, pp. 399–406 (August 1995)
4. Vanderborght, B., Albu-Schaeffer, A., Bicchi, A., Burdet, E., Caldwell, D.G., Carloni, R., Catalano, M., Eiberger, O., Friedl, W., Ganesh, G., Garabini, M., Grebenstein, M., Grioli, G., Haddadin, S., Hoppner, H., Jafari, A., Laffranchi, M., Lefeber, D., Petit, F., Stramigioli, S., Tsagarakis, N., Van Damme, M., Van Ham, R., Visser, L.C., Wolf, S.: Variable impedance actuators: A review. Robotics and Autonomous Systems 61(12), 1601–1614 (2013)

[1] An illustrative video of the experiment can be viewed at:
Human-operated control: `https://www.youtube.com/watch?v=y5nFrS6gnZQ`;
Human-like automatic control: `https://www.youtube.com/watch?v=C0gU6H2rChs`

5. Hogan, N.: Impedance control: An approach to manipulation. Journal of Dynamic Systems, Measurement, and Control 107(1), 8–16 (1985)
6. Burdet, E., Franklin, D., Milner, T.: Human Robotics - Neuromechanics and motor control. MIT Press (2013)
7. Ajoudani, A., Tsagarakis, N.G., Bicchi, A.: Tele-impedance: Teleoperation with impedance regulation using a body-machine interface. The International Journal of Robotics Research 31(13), 1642–1656
8. Potvin, J.R., Brown, S.H.M.: Less is more: High pass filtering, to remove up to 99% of the surface EMG signal power, improves emg-based biceps brachii muscle force estimates. Journal of Electromyography and Kinesiology 14(3), 389–399 (2004)
9. Baxter-research-robot. Baxter-research-robot profile, `http://www.rethinkrobotics.com/products/Baxter-research-robot/`
10. Smith, A., Yang, C., Ma, H., Culverhouse, P., Cangelosi, A., Burdet, E.: Bimanual Robotic Manipulation with Biomimetic Joint/Task Space Hybrid Adaptation of Force and Impedance. In: The Proceedings of the 11th IEEE International Conference on Control & Automation to be held in Taichung, Taiwan, June 18-20 (in press, 2014)
11. Osu, R., Franklin, D.W., Kato, H., Gomi, H., Domen, K., Yoshioka, T., Kawato, M.: Short-and long-term changes in joint co-contraction associated with motor learning as revealed from surface EMG. Journal of Neurophysiology 88(2), 991–1004 (2002)
12. Ajoudani, A., Tsagarakis, N.G., Bicchi, A.: Tele-impedance: Preliminary results on measuring and replicating human arm impedance in tele operated robots. In: 2011 IEEE International Conference on Robotics and Biomimetics (ROBIO), pp. 216–222 (December 2011)
13. Ray, G.C., Guha, S.K.: Relationship between the surface e.m.g. and muscular force. Medical and Biological Engineering and Computing 21(5), 579–586 (1983)
14. Wang, N., Yang, C., Lyu, M., Li, Z.: An EMG enhanced impedance and force control framework for telerobot operation in space. In: 2014 IEEE International Conference on Aerospace, pp. 1–12 (March 2014)